Effects of different Ga doping concentration on structural and optical properties of Ga–doped ZnO nanoparticles by precipitation reflux method

J Ungula*[1], F B Dejene[1] and H C Swart[2]

[1]Department of Physics, University of the Free State (QwaQwa Campus), Private Bag X13, Phuthaditjhaba, 9866, South Africa
[2]Department of Physics, University of the Free State, P.O Box 339, Bloemfontein 9300,
* Corresponding author E-mail: ungulaj@ufs.ac.za

Abstract. Ga-doped ZnO nanoparticles (GZO NPs) were synthesized by the precipitation reflux method. The effects of different Ga doping on the structural, morphological, luminescence and optical properties of GZO NPs were investigated for application as transparent conducting oxides. Structural crystallization was shown to improve with an increase in doping concentration up to 2 mol % as identified by X-ray diffraction. The scanning electron microscopy images showed that the grain sizes increased when increasing the Ga concentration up to 2 mol. % then reduced in size at higher doping concentrations (3-5 mol. %). Photoluminescence results revealed changes in emission peaks of GZO NPs with variation in levels of doping with the highest intensity of the excitonic peak at 2 mol. %. Reflectance of GZO NPs in the UV region was observed to increase up to 2 mol % doping and then reduced at higher doping as determined using an UV–Visible spectrometer. Likewise, an increase in optical band gap from 3.13 to 3.3 eV was observed as the doping concentration increased from 0 to 2 mol. %.

1. Introduction

Ga-doped ZnO (GZO) is an example of ZnO based transparent conducting oxides (TCO) being pursued in the recent time for use as photo anodes in dye-sensitized solar cells (DSSCs), due to its low resistivity, high transmittance, non-toxicity and resource availability [1]. Besides, research has shown that GZO has electrical and optical properties comparable to those of widely employed Indium Tin Oxide TCO and the performance of GZO TCO based DSSCs was found to be superior to fluorine-doped tin oxide based DSSCs under the same growing condition [2].

Doping into the ZnO lattice by replacing Zn^{2+} ions with higher valent ions such as Ga^{3+}, Al^{3+} and In^{3+} is one way to induce dramatic changes in the electrical and optical properties and to obtain thermally stable conductivity in ZnO for solar cells applications. Ga has a similar ionic radius and covalent radius (0.062 and 0.126 nm), as compared to those of Zn (0.074 and 0.134 nm), respectively [3, 4]. Thus, Ga^{3+} can be substituted for Zn^{2+} over a larger doping range compared to other metal dopants in its group, without any lattice distortion.

Many studies on GZO nanostructures have been reported, with many choosing 4 mol % GZO targets, and some others choosing 2, 3, or 5 mol % GZO to obtain thin films and other nanostructures,

which have excellent material properties [5–7]. Gomez and Olvera et al [8] reported a minimum electrical resistivity value of the order of 7.4×10^{-3} Ωcm and optical transparency of the order of 80 % at 2 mol. % targets. In spite of these reports, it still remains a challenge to achieve high quality of crystalline particles with excellent physical and chemical properties of GZO NPs.

A number of methods for the synthesis of GZO nanopowders have been investigated [9-11]. But unlike some which use complex processes to obtain the samples or demand very high power synthesis conditions in temperature or pressure that makes sizing up of the product a daunting challenge, the precipitation method offers several advantages, which include cost effectiveness, high purity, homogeneity and small crystalline size of its product [12].

In this work, we focus on the optimization of the Ga doping levels in GZO NPs in order to improve the structural, optical and luminescence properties as well as to ensure a large scope of transparency not only in the visible region but also in the near UV region using the precipitation reflux method. To the best of our knowledge, there are only handful of reports in the literature on the synthesis of GZO NPs using this method.

2. Experimental procedure

GZO NPs were synthesized with different Ga^{3+} concentrations. The chemical reagents sodium hydroxide (NaOH), zinc nitrate ($Zn(NO_3)_2$) and gallium nitrate hexahydrate ($Ga(NO_3)_3.6H_2O$) were of analytical grade and were used without further purification. In order to dope Ga in ZNPs, five different mol. % doping concentrations (0, 1, 2, 4 and 5) were selected. $Zn(NO_3)_2$ was mixed with ($Ga(NO_3)_3.6H_2O$), dissolved in ethanol solvent to make a 0.5 M solution and put in a three-neck glass flask. The solution in the flask was heated under continuous stirring to 70 °C. 10 mg of Polyvinylpyrrolidone was added as a surfactant to reduce agglomeration of nanoparticles during the growth while 2 ml acetic acid was added to ensure both total dissolution of zinc nitrate and to adjust precursor solution to pH of 5.8. A solution of 1 M NaOH was added slowly (dropped for 60 minutes) into the three-neck glass flask containing zinc nitrate-gallium nitrate solution and refluxed under continuous stirring. The suspension formed with the dropping of NaOH was kept stirred for two hours at the same growth temperature and allowed to stand overnight. The material was then filtered and washed several times with deionized water with a pH of 7.5. The washed sample was dried at 60 °C in an oven for one hour and packaged into sample containers.

The characterization of the samples was done by means of a scanning electron microscopy (SEM), energy dispersive X-ray spectroscopy (EDS), X-ray diffraction (XRD), UV-vis spectroscopy and Photoluminescence spectroscopy (PL).

3. Results and Discussion

3.1. XRD analysis

Figure 1(a) shows the XRD diffraction patterns of GZO NPs prepared with different mol. % of Ga^{3+} ions. The patterns consist of broad peaks, which match the common ZnO hexagonal wurtzite structure and are in agreement with the reported values (JCPDS card, No. 79-0205). The XRD results show only diffraction peaks of ZnO without any trace of other diffraction peaks such as $Zn_{1-x}Ga_xO_4$ and Ga_2O_3. The absence of impurity phases proved that all the gallium ions successfully substituted for the Zn sites in the ZnO lattice when doping ZnO with gallium in this study. This also reveals that it is plausible for the Ga^{3+} to reside on zinc sites in the hexagonal lattice [13]. The average dimensions of crystallite size 'D' were estimated from the values of 2θ and β of the XRD peaks using Scherrer's formula [14].

$$D = \frac{K\lambda}{\beta \cos\theta} \quad (1)$$

where, K is the shape factor, (K = 0.94), D is the crystallite size, β is the Full Width at Half Maximum, λ is the wavelength of X-rays used (1.5405 Å), and θ is the Bragg's diffraction angle.

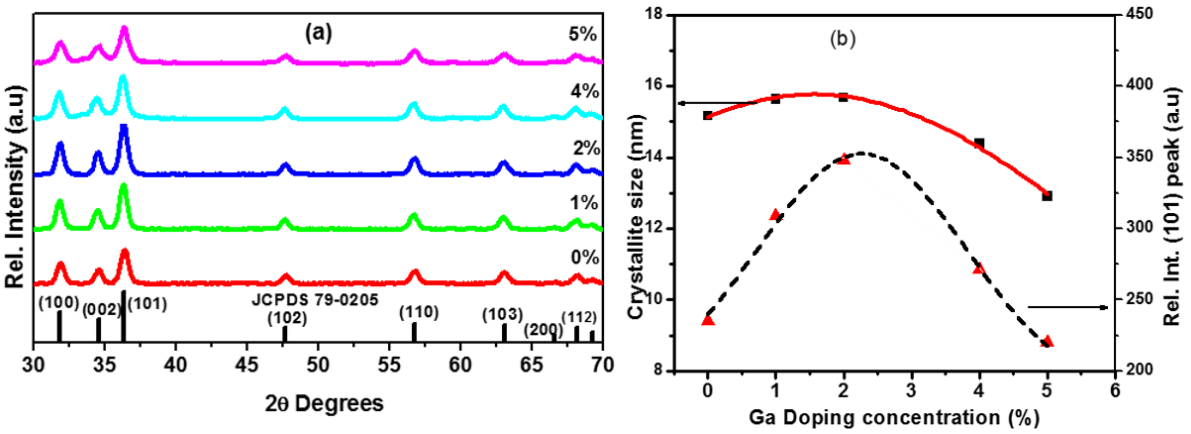

Figure 1: (a) X-ray powder diffraction patterns for GZO NPs prepared at different doping concentrations (b) Crystallite sizes and relative intensity of peak (101) as a function of Ga doping concentrations.

The crystallite sizes D and the relative intensity of peak (101) of the GZO NPs prepared at different concentration of the Ga dopant are plotted in figure 1(b). The D values are 15, 16, 16, 14 and 13 nm for 0, 1, 2, 4 and 5 mol. % doping, respectively. It was observed that a small amount of Ga atoms leads to the improvement in the crystalline quality and increase in crystallite size of the GZO NPs; as indicated by the highest value of D and peak intensity at the 2 mol % Ga doping concentration, but further increase in the Ga atoms results to a decrease in the intensity of the peaks and crystallite sizes. This may be due to the fact that up to 2 mol. % doping, Ga^{3+} ions replace the Zn^{2+} ions in the ZnO lattice but subsequent increase in doping levels may cause Ga^{3+} ions to occupy the interstitial positions in the ZnO lattice. Possibly, higher Ga doping levels could also weaken the crystallinity of GZO NPs due to the formation of stress by the smaller radius of Ga^{3+} ions (0.062 nm) compared with Zn^{2+} ions (0.074 nm).

3.2. SEM analysis

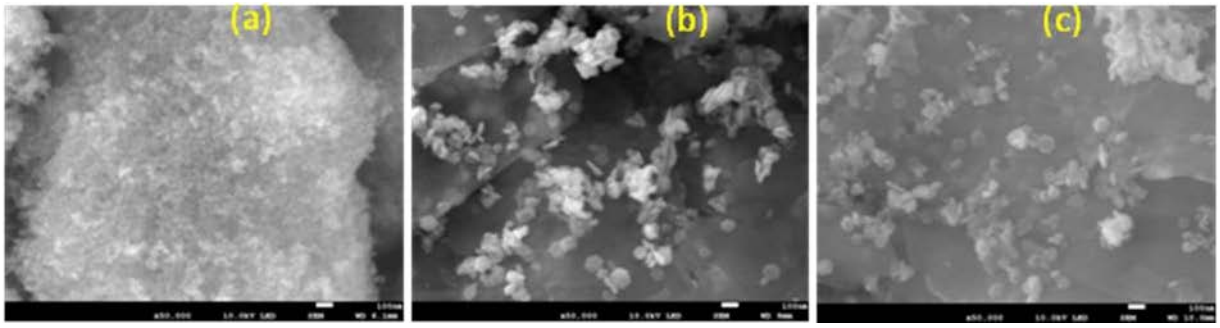

Figure 2: SEM micrographs of GZO NPs synthesized at (a) 0% (b) 2% and (c) 5% doping concentrations.

Figures 2(a-c) show the surface morphology images of the GZO NPs prepared at the different Ga doping concentrations (0, 2 and 5 mol. %). Agglomerated tiny spherical particles were formed at 0 mol. % doping which changed to less dense and dispersed larger hexagonal shaped NPs at 2 % doping. We attribute the reduced density to the formation of large grains as a result of coalescence of the particles with the increase in doping concentration. In the case of doping at 5 mol. % the grain size obtained decreased, which could be due to increasing number of nucleation sites, leading to the

formation of small grains during incorporation of the dopant into the host material [15]. The EDS images of the samples indicated that the collected powder was composed of zinc, oxygen and Ga and the synthesis route produced pure ZnO phases. This high purity of the GZO NPs was further confirmed by the XRD analysis.

3.3. Photoluminescence Analysis

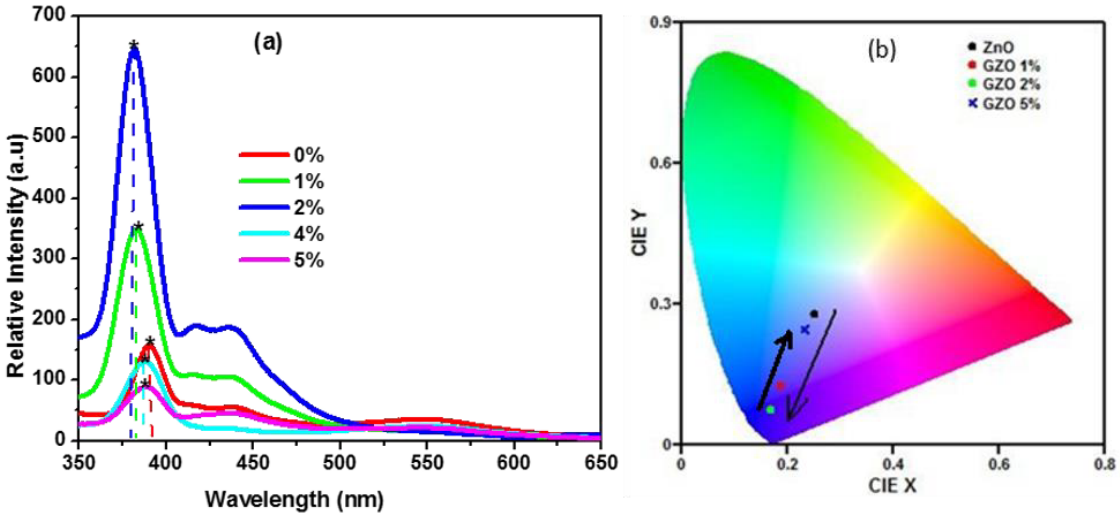

Figure 3: (a) PL emission spectra and (b) Chromaticity diagram depicting the CIE colour co-ordinates for GZO NPs for the different doping concentrations.

The PL spectra of GZO NPs for different Ga doping concentrations are shown in figure 3(a), illustrating the common UV-visible emission due to near band emission (NBE) and deep level defects (DLE) along with blue emission bands around 435 nm and violet peak centred at 415-420 nm. The sharp and strong UV NBE that formed between 380 and 390 nm originated from the free exciton recombination of GZO NPs, while the DLE emissions are associated with oxygen defects [16]. It is also seen, from figure 3(a), that the intensity of the NBE emission increased as the doping concentration increased from 0 to 2 % but reduced with further addition of the Ga dopant. The stronger NBE emission peak intensity in the PL indicates good optical properties of the ZnO NPs, which may be attributed to the reduced concentration of defects and improved crystallinity, in agreement with the XRD results and also as shown by the reduction of the DLE peak emission with an increase in doping concentration to 2 mol%. The quenching of the excitonic peak emission of the GZO NPs after 2 mol% Ga doping concentration was probably due to an enhanced bulk diffusion process, defect generation and migration as a result of the increase in amount of Ga in the ZnO lattice. The violet peak observed in most samples were slightly shifted to larger wavelengths and increased in intensity with the increase in doping concentration to 2 mol%. The source of this violet luminescence at 419 nm (2.96 eV) is probably due to radiative defects related to the interface traps existing at the grain boundaries and emitted from the radiative transition between this level and the valence band [17]. Jeong et al [18] also observed that the violet peak centred at 415–420 nm can be attributed to the Zn vacancies.

The Commission International de I'Eclairage (CIE) chromaticity diagram of the GZO NPs is shown in figure 3(b). The CIE (x, y) colour co-ordinates for 0, 1, 2, 4 and 5 % Ga doping concentrations are (0.25, 0.28), (0.19, 0.13), (0.17, 0.08), (0.28, 0.36) and (0.23, 0.25), respectively. The co-ordinates shift toward the shorter wavelength with the increase in mol % doping concentration but change to longer wavelengths for a further doping increase after 2 mol %. The blue shift of the co-

ordinates with an increase in amount of dopant in the sample is also supported by the PL spectra wavelength shifts.

3.4. Optical properties

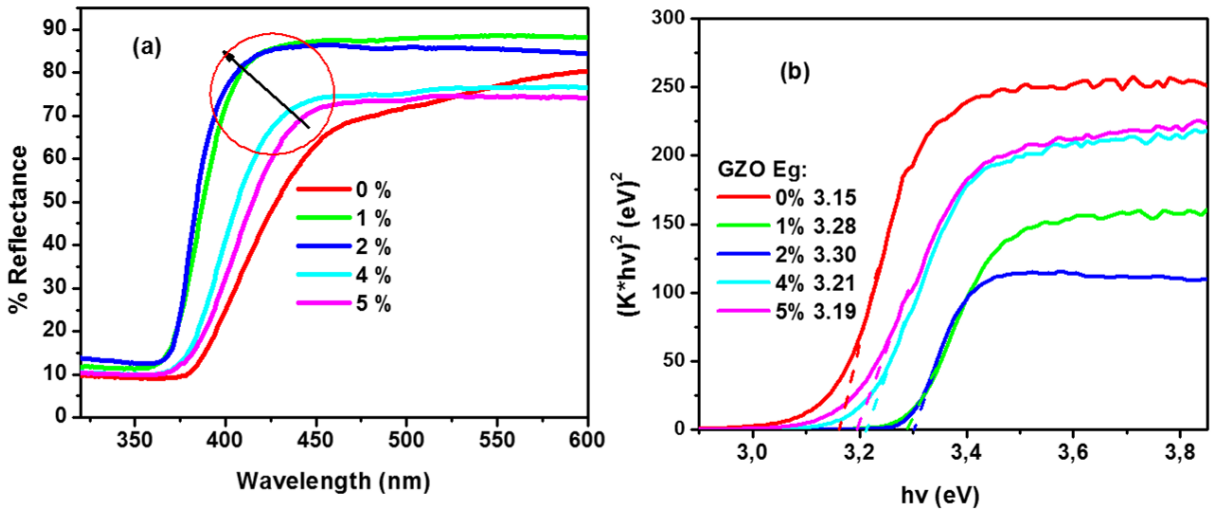

Figure 4: (a) The reflectance spectra and (b) Plot to determine the band gap energy of GZO nanoparticles prepared at various doping concentrations of Ga.

The reflectance spectra of the GZO NPs in the wavelength range of 300–600 nm are shown in figure 4(a). It can be observed that the onset of the band edge absorptions for the samples has blue shifted with the increase in doping concentration from 0 to 2 %, and red shifted with a further increase in the doping concentration confirming the size dependent absorption properties of the GZO NPs. Similarly, the % reflectance in the UV region has increased as the doping levels increased to 2 mol. %, but dropped as the concentrations increased to 5 mol %. Figure 4(b) shows the plot to determine the optical band gap of the ZnO NPs by extrapolating the linear region of the graph of the $(Khv)^2$versus *hv* graph near the onset of the absorption edge to the energy axis. The plots were obtained using the following equation [19].

$$(Khv)^2=A(hv-Eg)^2 \quad (2)$$

Where *K* is reflectance transformed according to the Kubelka-Munk remission function [20],

$$K=\frac{(1-R)^2}{2R} \quad (3)$$

hv is the photon energy, *Eg* is the optical band-gap energy between the valence band and the conduction band at n = 2 for direct transitions and A is a constant, depending on the electron–hole mobility and *R* is reflectance (%). The optical band gap was found to be 3.15, 3.28, 3.30, 3.21 and 3.19 eV corresponding to the Ga doping ratios of 0, 1, 2, 4, and 5 % respectively as shown in figure 4(b). The band gap values increased slightly with increasing Ga doping concentration to 2 mol %, and then decreased at higher doping. The highest optical band gap, 3.30 eV, was achieved in the GZO NPs doped with 2 mol % Ga due to the increase in carrier concentration, at this moderately doped level, caused by the contribution of Ga^{3+} ions at substitutional sites of Zn^{2+} ions and the higher energy-gap that resulted from the Ga interstitial atoms. The extrapolated absorption onset is slightly blue shifted on increasing the Ga doping concentration. This absorption edge which shifts towards higher energy is associated with an increase of the carrier concentration blocking the lowest states in the conduction band as explained by Burstein-Moss effect [21, 22].

4. Conclusions

The work in this investigation demonstrates that GZO NPs of high quality can be formed at a relatively low temperature (75 ºC) by precipitation reflux method by varying the Ga/Zn ratios. It was found that the crystallinity, surface morphology and optical properties of the GZO NPs depend strongly on the Ga doping levels. The XRD results established the synthesis process efficiency, showing only the hexagonal phase pattern and the nanometric behaviour of the crystallites formed. This result shows that GZO NPs prepared at 2 % Ga doping concentration exhibit the best crystal quality. Agglomerated tiny spherical particles were formed at 0 % doping which changed to less dense larger hexagonal shaped NPs at 2 % doping. It was seen that the intensity of the NBE emission increased as the doping concentration increased from 0 to 2 % but reduced with further doping indicative of the superior optical properties at 2 mol. % doping. The highest optical band gap, 3.30 eV, was also achieved in the GZO NPs doped with 2 mol % Ga due to the increase in carrier concentration, at this moderately doped level. The results of this work shows that a 2 mol % Ga-doped ZnO target is most suitable to obtain thin films with fairly good material properties for the use as a photo anode in DSSCs.

Acknowledgement

The financial support from the South African Research Chair Initiative (SARChI) bursary and University of the Free State is highly recognised.

References

[1] Netrvalova M, Novotny I, Prusakova L, Tvarozek V and Sutta P 2012 *Vacuum* 86 707–710
[2] Liu H, Avrutin V, Izyumskaya N, Özgür Ü and Morkoç H 2010 Superlattices and Microstructures 48(5) 458-484.
[3] Nayak P K, Yang J, Kim J, Chung S, Jeong J, Lee C and Hong Y 2009 *J Phys D: Appl Phys* **42** 035102.
[4] Yoshino K, Hata T, Kakeno T, Komaki H, Yoneta M, Akaki Y, Ikari T 2003 *Phys Stat Sol (c)* **0** 626.
[5] Jung K, Choi W K, Yoon S J, Kim H J and Choi J W 2010 *Applied Surface Science* **256** 6219.
[6] Miyake A, Yamada T, Makino H, Yamamoto N and Yamamoto T 2008 *Thin Solid Films* **517** 1037-1041.
[7] Nagarani S and Sanjeeviraja C 2011 *American Institute of Physics Conference Proceeding* **1349** 589-590.
[8] Gomez H and Olvera M de la L 2006 *Mater Sci Eng* B **134** 20–6.
[9] Du S, Tian Y, Liu H, Liu J, and Chen Y 2006 Journal of the American Ceramic Society 89(8) 2440-2443.
[10] Chen K J, Fang T H, Hung F Y, Ji L W, Chang S J, Young S J and Hsiao Y J 2008 Applied surface science 254(18) 5791-5795
[11] Guo J, Zheng J, Song X and Sun K 2013 Materials Letters 97 34-36.
[12] Chongsri K and Pecharapa W 2015 Integrated Ferroelectrics 165(1) 159-166
[13] Zhang D H, Yang T L, Ma J, Wang Q P, Gao R W and Ma H L 2015 Materials Research Express 2 9.
[14] Wagner R S and Doherty C 1996 *J Electroceram Soc* **113** 1300 3 4596.
[15] Hu J and Gordon RG 1992 *J Appl Phys* **72** 5381.
[16] Lin B and Fu Z 2001 *Appl Phys Lett* **79** 943.
[17] Jin B J, Im S and Lee S Y 2000 *Thin Solid Films* **366** 107-110.
[18] Jeong S H, Kim B S and Lee B T 2003 *Appl Phys Lett* **82** 2625.
[19] Tauc J, Grigorovichi R and Vancu A 1966 *Phys Status Solidi* **15** 627.
[20] Duran P, Capel F, Tartaj J and Moure C 2002 *Adv Mater* **14** 137.
[21] Burstein E 1954 *Physical Review* **93** 632-633.
[22] Moss T S 1954 *Proceedings of the Physical Society Section B* **67** 775.